

Accepted Manuscript

Structure and mechanical properties of sodium and calcium caseinate edible active films with carvacrol

Marina P. Arrieta, Mercedes A. Peltzer, María del Carmen Garrigós, Alfonso Jiménez

PII: S0260-8774(12)00428-1

DOI: <http://dx.doi.org/10.1016/j.jfoodeng.2012.09.002>

Reference: JFOE 7079

To appear in: *Journal of Food Engineering*

Received Date: 4 July 2012

Revised Date: 6 September 2012

Accepted Date: 8 September 2012



Please cite this article as: Arrieta, M.P., Peltzer, M.A., Garrigós, a.d.C., Jiménez, A., Structure and mechanical properties of sodium and calcium caseinate edible active films with carvacrol, *Journal of Food Engineering* (2012), doi: <http://dx.doi.org/10.1016/j.jfoodeng.2012.09.002>

This is a PDF file of an unedited manuscript that has been accepted for publication. As a service to our customers we are providing this early version of the manuscript. The manuscript will undergo copyediting, typesetting, and review of the resulting proof before it is published in its final form. Please note that during the production process errors may be discovered which could affect the content, and all legal disclaimers that apply to the journal pertain.

30 interactions between the protein matrix and glycerol, as it was also observed in thermal
31 degradation studies. FTIR spectra of all films showed the characteristic bands and
32 peaks corresponding to proteins as well as to primary and secondary alcohols. In
33 summary, the best results regarding mechanical and structural properties for
34 caseinates-based films containing carvacrol were found for the formulations with high
35 glycerol concentrations.

36

37 **Keywords:** edible films; caseinates; glycerol; carvacrol; active packaging.

38

39 1. INTRODUCTION

40 An increasing proactive attitude of society towards a reduction on the
41 environmental impact produced by food packaging after use is currently growing. This
42 could be joined to the consumer's demand for higher quality and longer shelf life food
43 with an increase on research in new active packaging formulations. Under this general
44 framework, the research on biopolymer-based packaging materials is being extensively
45 explored (Juvonen et al., 2011; Verbeek and Van den Berg, 2010). Another raising
46 tendency in food packaging research is the study of interactions between materials and
47 foodstuff to take advantage of the controlled migration of active additives. Some of
48 them can be extracted from essential oils obtained from aromatic plants with
49 antimicrobial activities (Chalier et al., 2007; Peltzer et al., 2009). They can be used to
50 control spoilage and pathogens proliferation in food during storage and distribution
51 (Ben Arfa et al., 2007; Moreira et al., 2011; Viuda-Martos et al., 2007). Antimicrobial
52 agents can be added by coating onto the food surface or could be incorporated into
53 food-packaging materials with controlled migration to foodstuff (Kristo et al., 2008).

54 The coordination of both concepts (i.e. sustainability and active packaging)
55 could result in the development of edible films with antimicrobial properties to be used
56 in food packaging materials (Ponce et al., 2008; Quintavalla and Vicini, 2002). In this
57 sense, carvacrol, a volatile aromatic compound extracted from oregano and thyme

58 essential oils, is well known for its antimicrobial activity (Lu et al., 2011; Mascheroni et
59 al., 2010; Nostro et al., 2007; Viuda-Martos et al., 2010; Viuda-Martos et al., 2011;
60 Viuda-Martos et al., 2007). Oregano oil has been widely used as a dietary supplement
61 for combating infections and relieving digestive and skin-related problems (Cho et al.,
62 2012).

63 The use of biopolymers as matrices in active packaging systems has been
64 relatively unexplored despite their sustainability and advantageous properties. For
65 instance, proteins are adequate for the preparation of biofilms by their high plasticity
66 and elasticity (Pereda et al., 2008; Pereda et al., 2011). In addition, they are abundant
67 in Nature and fully renewable (Ponce et al., 2008) since they can be obtained from
68 plants (corn zein, wheat gluten, soy or sunflower) and animal sources (gelatin, keratin,
69 casein or whey) (Hernandez-Izquierdo and Krochta, 2008; Verbeek and Van den Berg,
70 2010). Among them, caseinates can be considered attractive for their use in food
71 packaging, since they show numerous functional properties, such as water solubility
72 and ability to act as emulsifiers (Fabra et al., 2009; Jimenez et al., 2012; Pereda et al.,
73 2010). In addition, due to the high number of polar groups in their structure, caseinates
74 also show good adhesion to different substrates making them excellent barrier to non-
75 polar substances, such as oxygen, carbon dioxide and aromas (Audic et al., 2003).
76 However, due to the inherent brittleness of many biopolymers including caseinates,
77 plasticizers should be necessarily used to improve their ductile properties and to get
78 the flexibility required for films manufacturing (Martino et al., 2009). In this sense, the
79 use of glycerol has been proposed, since it contributes to the reduction in material
80 brittleness by the limitation of crosslinking and elimination of intra and intermolecular
81 hydrogen bonds (Pereda et al., 2008)). Furthermore, it should be pointed out that
82 glycerol is a by-product of biodiesel production; so, it would be positive to increase its
83 added value from a low-grade by-product to a useful plasticizer (Ye et al., 2012).

84 Some studies have been recently performed with casein and caseinates as
85 matrices for edible films. For instance, nano-biocomposites based on casein and

86 sodium montmorillonites were recently studied (Pojanavaraphan et al., 2010). Other
87 authors used modified sodium caseinate as matrix for edible films containing oleic acid-
88 beeswax mixtures (Fabra et al., 2009) or tung oil (Pereda et al., 2010). Antimicrobial
89 edible films were also obtained from sodium caseinate and chitosan blends (Pereda et
90 al., 2008) or nisin (Cao-Hoang et al., 2010). In this work we compare two commercial
91 caseinates in their use as matrices form polymer edible films. Carvacrol was chosen as
92 antimicrobial agent in these formulations since this compound presents several positive
93 characteristics. It is a natural compound with antimicrobial activity against a broad
94 range of bacteria and it is categorized as GRAS (FDA Admistration US). Carvacrol has
95 been recently used as active additive in different formulations for active packaging with
96 promising results (Gutierrez et al., 2010; Persico et al., 2009; Ramos et al., 2012).
97 However, at the best of our knowledge the addition of carvacrol into sodium or calcium
98 caseinates for edible films manufacturing has not been reported.

99 The aim of the present work is the development of carvacrol edible active films
100 based on sodium and calcium caseinates plasticized with glycerol. Films were obtained
101 by solvent casting and further characterized to evaluate their viability for food
102 packaging applications, regarding their structure, mechanical and thermal properties.

103

104 **2. EXPERIMENTAL**

105 **2.1 Materials**

106 Sodium (SC) and calcium caseinates (CC) were kindly supplied in powder form
107 by Ferrer Alimentación S.A (Barcelona, Spain). Carvacrol (98%) and anhydrous
108 glycerol (99.5%) were purchased from Sigma Aldrich (Móstoles, Madrid, Spain).

109

110 **2.2 Films preparation**

111 Films were prepared by solvent casting. Solutions were prepared in distilled
112 water with 5 wt% of caseinate, either SC or CC. Glycerol was added to obtain
113 protein:glycerol ratios 1:0, 1:0.15, 1:0.25, 1:0.35. Solutions were then heated at 65 °C

114 for 10 minutes under continuous stirring at 1100 rpm and further cooled at room
115 temperature. The final pH of these caseinates-glycerol solutions was 6.95.
116 Furthermore, carvacrol was added at 10 wt% resulting in a final protein:carvacrol ratio
117 1:0.10, with homogenization for 3 min at 1100 rpm. The pH of these solutions was
118 between 5.35 and 5.40. Finally, ultrasonic degasification at room temperature was
119 applied to all solutions to eliminate foams and air bubbles.

120 Films were prepared by taking 30 mL of these solutions into 15-cm diameter
121 polyethylene Petri dish containers (Distrilab S.L., Cartagena, Spain). They were
122 conditioned at 25 ± 2 °C and 50% constant relative humidity (RH) in a Dycometal-
123 CM81 climatic test chamber (Barcelona, Spain) for 48 h.

124 The average thickness of films was measured with a Digimatic Micrometer
125 Series 293 MDC-Lite (Mitutoyo, Japan) ± 0.001 mm at ten random positions over the
126 film surface.

127 128 **2.3. Characterization**

129 Thermogravimetric analysis (TGA) tests were carried out by using a TGA/SDTA
130 851 Mettler Toledo thermal analyzer (Schwarzenbach, Switzerland). Samples weighing
131 around 5-10 mg were heated from room temperature to 700 °C at $10^\circ \text{C min}^{-1}$ under
132 nitrogen atmosphere (50 mL min^{-1}) and from 700 °C to 900 °C at the same heating rate
133 under oxygen atmosphere (50 mL min^{-1}) with the aim of determining the inorganic
134 residue in each formulation. The initial degradation temperature (T_0) was calculated at
135 10% mass loss, while temperatures at the maximum degradation rate (T_{max}) for each
136 stage were determined from the peaks of the derivative curves (DTG).

137 Fourier transformed infrared spectroscopy (FTIR) tests were carried out by
138 using a Perkin-Elmer infrared spectrometer (Perkin Elmer Spain, S.L., Madrid Spain).
139 Samples were cut in 1cm x 1cm squares, with average thicknesses 88 ± 16 μm for SC
140 and 103 ± 11 μm for CC films, and were analysed at room temperature and 50% RH.
141 Attenuated total reflectance (ATR) spectra were obtained in the $4000\text{-}600 \text{ cm}^{-1}$ region,

142 using 128 scans and 4 cm⁻¹ resolution. A blank spectrum was obtained before each
143 test to compensate the humidity effect and the presence of carbon dioxide in the air by
144 spectra subtraction.

145 Samples surfaces were observed by an optical microscopy (Olympus BH2-UMA
146 Microscope), with no further preparation, by ordinary light.

147 Scanning electronic microscopy (SEM) surface and cross section tests were
148 carried out with a JEOL JSM-840 microscope (Jeol USA Inc., Peabody, USA),
149 operated at 10 kV. 10 x 10 mm² samples were cut and coated with gold layer (10-25
150 nm) prior to analysis in order to increase their electrical conductivity. Images were
151 registered at 1000x magnification.

152 Tensile tests were carried out at room temperature and 50% RH by using a
153 3344 Instron Instrument (Fareham Hants, UK) according to ASTM D882-01 Standard
154 (ASTM, 2001). Tests were performed in rectangular strips (10 x 100 mm²), initial grip
155 separation 50 mm and crosshead speed 25 mm min⁻¹. Average percentage
156 deformation at break (ϵ_B %), elastic modulus (E) and tensile strength (TS) were
157 calculated from the resulting stress-strain curves as the average of five measurements
158 from three films of each composition.

159

160 **3. RESULTS AND DISCUSSION**

161 Transparent SC and CC edible films were successfully obtained by following the
162 above-described procedure. No apparent differences in transparency and colour can
163 be reported for samples containing carvacrol after comparison with the non-active
164 counterparts (Figure 1). However, samples containing carvacrol showed a slightly
165 characteristic oregano odor. Average thicknesses were 88 ± 16 μm for SC and 103 ±
166 11 μm for CC films.

167

168 **3.1 Thermal properties**

169 Table 1 and 2 summarize the TGA results for the SC and CC edible films,
170 respectively. Pure SC and CC showed similar degradation patterns, with two main
171 thermal events. The first one was observed around 120-140 °C corresponding to the
172 evaporation of absorbed and bound water in caseinates structure. The second stage
173 was associated to their degradation and it was observed from 189 °C (T_0) for SC and
174 198 °C (T_0) for CC, reaching T_{max} at 330 °C and 338 °C, respectively. The residue at
175 700 °C was around 25% in both cases.

176 Pure glycerol showed a single degradation step, with T_0 146 °C and T_{max} 269 °C.
177 No residue at 700 °C was observed. On the other hand, carvacrol degraded in two
178 steps, with T_{max} at 92 °C and 208 °C. The residual waste after degradation at 700 °C
179 was negligible.

180 In general terms, TGA curves for films showed more than one degradation step.
181 Non-plasticized films (i.e. pure SC and CC) showed the same TGA pattern than the
182 original powder. Nevertheless, it should be noted that caseinate/glycerol blends
183 showed lower decomposition temperatures than non-plasticized films, indicating a
184 decrease in thermal stability caused by the presence of plasticizer. This result can be
185 explained by the influence of glycerol on the reduction in the number of inter and
186 intramolecular bonds in the protein structure, resulting in a decrease of thermal stability
187 of the whole system (Barreto et al., 2003).

188 On the other hand, plasticized films with carvacrol showed three degradation
189 steps (Figure 2). The first event was observed at temperatures around 100 °C and it
190 was related to the loss of moisture and bound water remaining from the casting
191 process. The second stage at temperatures between 200 °C and 250 °C could be
192 related to the loss of glycerol and carvacrol from the material. A similar behaviour was
193 described by other authors indicating that glycerol can be easily eliminated from
194 caseinate films at temperatures between 105-239 °C (Pereda et al., 2008). Finally, the
195 third degradation process, at temperatures above 300 °C, was associated to the
196 protein thermal degradation. This sequential degradation of these films during heating

197 could be explained by the gradual loss of the initial ordered structure of the polymer
198 matrix, since inter and intra-molecular hydrogen bonding are broken up at raising
199 temperatures (Barreto et al., 2003). As it has been reported, the presence of additives
200 in these formulations contributes to the decrease in the number of protein-protein
201 bonds, resulting in lower thermal stability of these samples (Verbeek and Van den
202 Berg, 2010). In general CC films showed higher thermal stability than those based on
203 SC. This result could be explained by considering that divalent calcium cations in CC
204 promote cross-linking with protein chains, giving rise to a more rigid structure with
205 higher thermal stability (Fabra et al., 2010).

206 However, in CC films the presence of carvacrol had no influence on protein-
207 protein bonds since the maximum degradation temperature remained nearly constant
208 for all films. As expected, it was observed that the T_0 decreased with the addition of
209 higher amounts of glycerol in SC and CC films indicating a good incorporation of the
210 plasticizer to the polymer matrix.

211

212 **3.2 FTIR analysis**

213 **3.2.1 Raw materials**

214 Molecular interactions in blends were studied by obtaining their FTIR spectra.
215 The analysis of films obtained from raw materials was performed and results for
216 glycerol and carvacrol as well as for SC and CC in powder form are shown in Figure 3.
217 The spectrum for glycerol (Figure 3a) shows the typical bands for alcohols, with the
218 stretching absorption associated with the hydroxyl groups (-OH) in the $3600-3000\text{ cm}^{-1}$
219 range, while the carbon-oxygen (C-O) absorption peaks characteristic of primary and
220 secondary alcohols were observed at 1030 and 1100 cm^{-1} , respectively. In addition,
221 peaks for CH-OH bending were observed at $1125-1100\text{ cm}^{-1}$, while $\text{CH}_2\text{-OH}$ bending
222 bands appeared at $1075-1000\text{ cm}^{-1}$. Bands in the $1400-1200\text{ cm}^{-1}$ range can be
223 assigned to the in-plane bending of the hydroxyl group. Finally, asymmetric and

224 symmetric stretching vibrations associated with carbon-hydrogen (C-H) bonds were
225 identified at 2875 cm^{-1} and 2925 cm^{-1} , respectively (Pretsch, 2001).

226 The spectrum for carvacrol (Figure 3b) also showed wide stretching absorption
227 bands associated to the -OH stretching region from 3650 to 3100 cm^{-1} . Peaks
228 observed between 1600 and 1400 cm^{-1} could be attributed to the aromatic ring
229 insaturations in the carvacrol molecule, particularly to in-ring carbon-carbon stretching.
230 Stretching vibration peaks for the aromatic hydroxyl groups were identified around
231 1250 cm^{-1} . Out of plane stretching peaks due to aromatic C-H bonds were observed in
232 the $900\text{-}650\text{ cm}^{-1}$ range. Asymmetric and symmetric stretching vibrations of C-H bonds
233 (2867 cm^{-1}), symmetric stretching of -CH_3 (1380 cm^{-1}) and bending of -CH_3 (1340 cm^{-1})
234 were also assigned. Finally, the aromatic C=C stretching was identified at 800 cm^{-1} .
235 Overtones characteristic of aromatic compounds were present as weak bands in the
236 $2000\text{-}1665\text{ cm}^{-1}$ region (Pretsch, 2001).

237 The spectra for caseinates (Figure 3e) showed strong amide I and amide II
238 peaks between $1700\text{-}1500\text{ cm}^{-1}$ and the -NH group stretching at $3400\text{-}3000\text{ cm}^{-1}$
239 characteristic of amino acids, as it was previously reported by other authors (Oliver et
240 al., 2009; Pereda et al., 2008). A small shoulder at 3080 cm^{-1} could be assigned to the
241 primary amines structure, being probably an overtone of the amide II absorption peak
242 (Pereda et al., 2008). Peaks at 1630 cm^{-1} in the amide I region and 1510 cm^{-1} in the
243 amide II region could be assigned to the stretching of the carbonyl group (C=O) and to
244 the symmetric stretching of N-C=O bonds, respectively. The bands around 1400 cm^{-1}
245 could be assigned to the carboxylate group (O-C-O) (Abu Diak et al., 2007). The
246 bands at 1174 cm^{-1} and 1066 cm^{-1} for SC and at 1160 cm^{-1} and 1091 cm^{-1} for CC
247 resulted from the C-O stretching in C-OH bonds (Pelissari et al., 2009). The most
248 important differences between the spectra for SC and CC in powder were found at low
249 wavenumbers (Figures 3e). In agreement with results reported by other authors
250 (Pelissari et al., 2009; Wang et al., 2007), SC had the C-O stretching band in C-OH at
251 1076 cm^{-1} , while CC showed these bands at 1090 and 1156 cm^{-1} . It was reported that

252 monoanionic phosphates showed symmetric stretching bands around 1080 cm^{-1} while
253 the same band appeared at 976 cm^{-1} in dianionic phosphates (Fernandez et al., 2003).
254 In this study, SC showed a band at 974 cm^{-1} and CC at 995 cm^{-1} suggesting
255 monocationic and dicationic interactions with Na^+ and Ca^{+2} , respectively.

256

257 **3.2.2 SC, CC, SC/G/CRV and CC/G/CRV edible films**

258 FTIR spectra corresponding to the SC powder, G and SC films with different
259 glycerol concentrations in the $3600\text{--}2800\text{ cm}^{-1}$ range (corresponding to -OH and -NH
260 stretching bands) are shown in Figure 4a. Due to the caseinates random coil nature
261 and their ability to form extensive intermolecular hydrogen bonds, their blending with
262 glycerol resulted in a general increase in the macromolecules cohesion (Avena
263 Bustillos and Krochta, 1993). Thus, the broad absorption band observed in the 3600--
264 3000 cm^{-1} range can be attributed to hydrogen bonds formed between SC and glycerol
265 hydroxyl groups (Barreto et al., 2003; Pelissari et al., 2009) as well as to the presence
266 of unbonded N-H groups (Barreto et al., 2003; Pereda et al., 2008). As expected, the
267 intensity of this broad band increased with the glycerol concentration since the number
268 of available hydroxyl groups was proportionally higher. Similar comments could be
269 applied to the asymmetric and symmetric stretching vibrations of C-H bonds at 2875
270 and 2925 cm^{-1} . Similar spectra were obtained for CC-based films (not shown). The
271 intensity of the amide I band (1630 cm^{-1}) decreased when the glycerol percentage
272 increased, as expected due to the lower proportion of protein in the final formulation.
273 On the other hand, the band indicative of the amide II group shifted from 1510 to 1530
274 cm^{-1} . This effect could be associated to the existence of conformational
275 rearrangements in the protein caused by the addition of glycerol, resulting in the
276 decrease of inter- and intra-molecular hydrogen bonding. In addition, the intensity of
277 these bands decreased with the increasing concentration of glycerol by the formation of
278 -N-OH bonds, resulting in the reduction of free amine groups. Similar spectral changes
279 were observed for the amide I band in caseinate/sorbitol films (Barreto et al., 2003). In

280 this sense, other bands related to the amide group (1440 and 1390 cm^{-1}) showed lower
281 intensities when glycerol concentration increased, while, higher intensities in those
282 bands characteristic of primary and secondary alcohols (1030 and 1100 cm^{-1}) were
283 observed when glycerol concentration increased (Figure 4b). This trend can be
284 qualitatively corroborated since qualitative data can be obtained by using the
285 relationship between two peaks areas (Arrieta et al., 2012). Therefore, in order to
286 obtain a qualitative assessment of the effect of glycerol concentration on these films,
287 the relationship between of the areas of amida I peak (1630 nm) and the primary
288 alcohol peak (1030 nm), was then calculated as amide I: alcohol 1° . Therefore, by
289 comparing results of amide I: alcohol 1° ratio shown in Table 3, it could be concluded
290 that it increased with the concentration of glycerol in both matrices, corroborating the
291 interactions between glycerol and caseinates. Similar results were described for blends
292 of α - and β -casein with tea polyphenols (Hasni et al., 2011). Figure 4c shows the
293 spectra of carvacrol active films. As expected from the pure CRV spectrum (Figure 3b),
294 formulations with this additive showed a strong wide band for O–H stretching in the
295 3600 - 3100 cm^{-1} region, as well as a multiband pattern in the 3100 - 2800 cm^{-1} range,
296 overlapping with OH- and NH- stretching bands of caseinates and glycerol. However,
297 some slight differences in a band centered at approximately 3300 cm^{-1} were noted,
298 since its intensity was lower with the addition of carvacrol to both caseinates. This
299 result suggests a reduction in the hydrophilic character of films. Similar results were
300 found after the addition of tung oil to SC films (Pereda et al., 2010).

301 Other significant differences in FTIR spectra for films with and without CRV
302 could be observed in the 1200 - 600 cm^{-1} region (Figure 4 d), where several peaks were
303 detected in samples with carvacrol corresponding to phenolic bonds. Their presence
304 gives an indication of the effective incorporation of the active additive to the biopolymer
305 matrices.

306

307 **3.3 Microstructure of edible films**

308 The obtained films were mostly homogeneous in their surface with no apparent
309 phase separation as evidenced from optical and SEM observations. Optical
310 micrographs of films with CRV showed some droplets (Figure 5). The presence of
311 these droplets can be attributed to the hydrophobicity of carvacrol that constitutes an
312 emulsion in the caseinate-glycerol aqueous solution. However, some differences
313 between SC and CC emulsions were observed. These differences could be explained
314 by the relationship between α and β -caseins and the aggregation of each protein. α -
315 casein is associated in a series of consecutive steps whereas the association of β -
316 casein shows detergent-like micellization (Srinivasan et al., 1999). At the protein
317 concentration level used in this work (5 wt%), both SC and CC showed preferential
318 absorption of α -casein to the droplet surfaces. However, it can be observed that
319 droplets in CC-CRV edible films (Figure 5d) were slightly larger than droplets in SC-
320 CRV edible films (Figure 5b). These observations may be due to the fact that surface
321 protein loads were higher in calcium caseinate emulsions due to the presence of large
322 aggregates of protein (Srinivasan et al., 1999).

323 Figure 6 shows SEM micrographs of unplasticized CC film (Figure 6a) and
324 plasticized with 35 wt% of glycerol (Figure 6b), both with 10 wt% CRV in their
325 formulations. Other authors reported also homogeneous and smooth surfaces for
326 caseinate films, particularly those with CC (Gastaldi et al., 2007) and SC/G (Fabra et
327 al., 2009; Pereda et al., 2010). In this work no significant differences were noticed in
328 sample surfaces by the addition of CRV, indicating a good dispersion of the
329 antimicrobial agent in the unplasticized and plasticized matrices. Similar results were
330 reported for coating paper based on soy protein and carvacrol (Chalier et al., 2007).

331 Figure 7 shows SEM micrographs taken to the cross section of unplasticized
332 SC (Figure 7a), films plasticized with 35 wt% glycerol (Figure 7b), films plasticized SC
333 containing CRV (Figure 7c) and unplasticized CC containing CRV (Figure 7d). In all
334 cases, some small holes were observed due to the bubbles bursting through the
335 surface during the casting process when water vaporization occurred (Chalier et al.,

2007). No apparent phase separation was observed in plasticized samples. This result indicates that regardless of the amount of plasticizer used in formulations, glycerol well incorporated to the protein matrix.

339

340 **3.4. Mechanical properties**

341 Differences in tensile properties between SC and CC films with glycerol
342 incorporated at several concentrations as well as the influence of carvacrol on their
343 ductile behaviour were evaluated. Tables 4 and 5 show results obtained for the elastic
344 modulus (E), tensile strength (TS) and elongation at break ($\epsilon\%$). In general terms,
345 unplasticized films were fragile and they cracked while clamping before testing.
346 Therefore, tensile properties were not possible to be calculated for such formulations.
347 CC-based films showed higher E and TS values and lower $\epsilon\%$ than their SC
348 counterparts. Therefore, SC films offer more flexible structures than CC-based
349 materials. These results are in good agreement with Fabra et al. (2010), who claimed
350 that the substitution of SC by CC results in an increase of stiffness and resistance to
351 break in caseinate films.

352 As expected, the plasticization process caused a significant decrease in E
353 values for all formulations. It could be observed that $\epsilon\%$ increased with the amount of
354 glycerol, particularly for 35 wt% formulations, as expected for plasticized polymers.
355 This parameter also increased with the addition of carvacrol for films based on SC and
356 CC plasticized with 25 wt% of glycerol. These results demonstrated that carvacrol
357 affect in some way the interactions between macromolecular chains in the polymer
358 matrix, as previously indicated in the TGA study. This effect may be related to
359 electrostatic interactions between caseinates and the active agent due to the different
360 charge distribution into the protein chains. It can be stated that caseinates act as
361 macroanions at the experimental pH. If considering that the pK_a of phenolic compounds
362 such as carvacrol is around 10, the hydroxyl group should be present (Ultee et al.,

363 2002). These authors proposed that carvacrol could be a proton carrier by exchanging
364 its hydroxyl proton for another cation, such as positively-charged potassium. Therefore,
365 the exchange of the hydroxyl proton in carvacrol by mono- or dications could be the
366 reason why CC gave more rigid structures. Other authors reported that oleic acid
367 interactions with caseinates were reduced when calcium caseinate was added in
368 sodium caseinate films (Fabra et al., 2010).

369 It is known that, in general terms, films for packaging require high flexibility at
370 room temperature to avoid unnecessary breaking during processing and use (Martino
371 et al, 2006). In this sense, it was demonstrated that the formulation of sodium
372 caseinate plasticized with 35 wt% of glycerol and 10 wt% of carvacrol (SC-G35-CRV)
373 showed the most adequate mechanical response for food contact films, with increased
374 flexibility to ensure processing and further use while containing the antimicrobial agent
375 to be used in active packaging formulations.

376

377 **Conclusions**

378 Transparent and homogeneous edible films based on SC, CC, SC/CRV and
379 CC/CRV plasticized with three different glycerol concentrations were successfully
380 obtained and characterized in terms of their structure, thermal and mechanical
381 properties. CC edible films showed higher thermal stability than SC counterparts, due
382 to the presence of divalent calcium cations promoting cross-linking with protein chains
383 giving a more rigid structure, as it was also proved in tensile testing. The addition of
384 CRV did not influence significantly the thermal stability of CC films. However, thermal
385 stability slightly decreased for SC edible films including CRV. FTIR spectra showed that
386 glycerol is strongly bound to caseinates, in particular when the number of hydroxyl
387 groups increases at high glycerol concentrations. Caseinate-carvacrol interactions
388 could suggest that the resulting materials could have more hydrophobic character than
389 those materials without the active agent. Optical microscopy observations are in close
390 accordance with the hydrophobic character suggested for caseinate-carvacrol

391 formulations, where stable emulsions are formed. Regarding mechanical properties,
392 SC edible films showed higher flexibility than their CC counterparts. Ductile properties
393 of films improved with the addition of glycerol, but some caution should be necessary to
394 avoid phase separation and the consequent migration of plasticizer to foodstuff.

395 Therefore, it can be concluded that glycerol and carvacrol showed good
396 compatibility with caseinates to form homogeneous films. Among all the tested
397 formulations, the best results were found for materials with carvacrol incorporated at 10
398 wt% and glycerol at 35 wt %. This formulation ensures conditions for film processing as
399 well as the significant presence of an antimicrobial additive to get an active packaging
400 system. Consequently, these edible films show potential for their future use in fresh
401 food preservation. Furthermore, more studies on functional properties related to food
402 contact materials (i.e. permeability to gases, water vapour permeability, migration in
403 different environments and antimicrobial properties) as well as the biodegradable
404 characteristics of these formulations should be necessary and are currently on- going.

405

406 **Acknowledgments**

407 Marina Patricia Arrieta thanks Fundación MAPFRE for “Ignacio Hernando de
408 Larramendi 2009- Medio Ambiente” fellowship (MAPFRE-IHL-01). The Spanish
409 Ministry of Economy and Competitiveness is acknowledged by financial support
410 (project Ref. MAT2011-28468-C02-01). Authors thank to Ferrer Alimentación S.A., for
411 providing caseinates and to Prof. Juan López Martínez (Polytechnic University of
412 Valencia, Spain) for his collaboration and useful discussions.

413

414 **References**

415 Abu Diak, O., Bani-Jaber, A., Amro, B., Jones, D., Andrews, G.P., (2007). The
416 manufacture and characterization of casein films as novel tablet coatings. Food and
417 Bioproducts Processing 85(C3), 284-290.

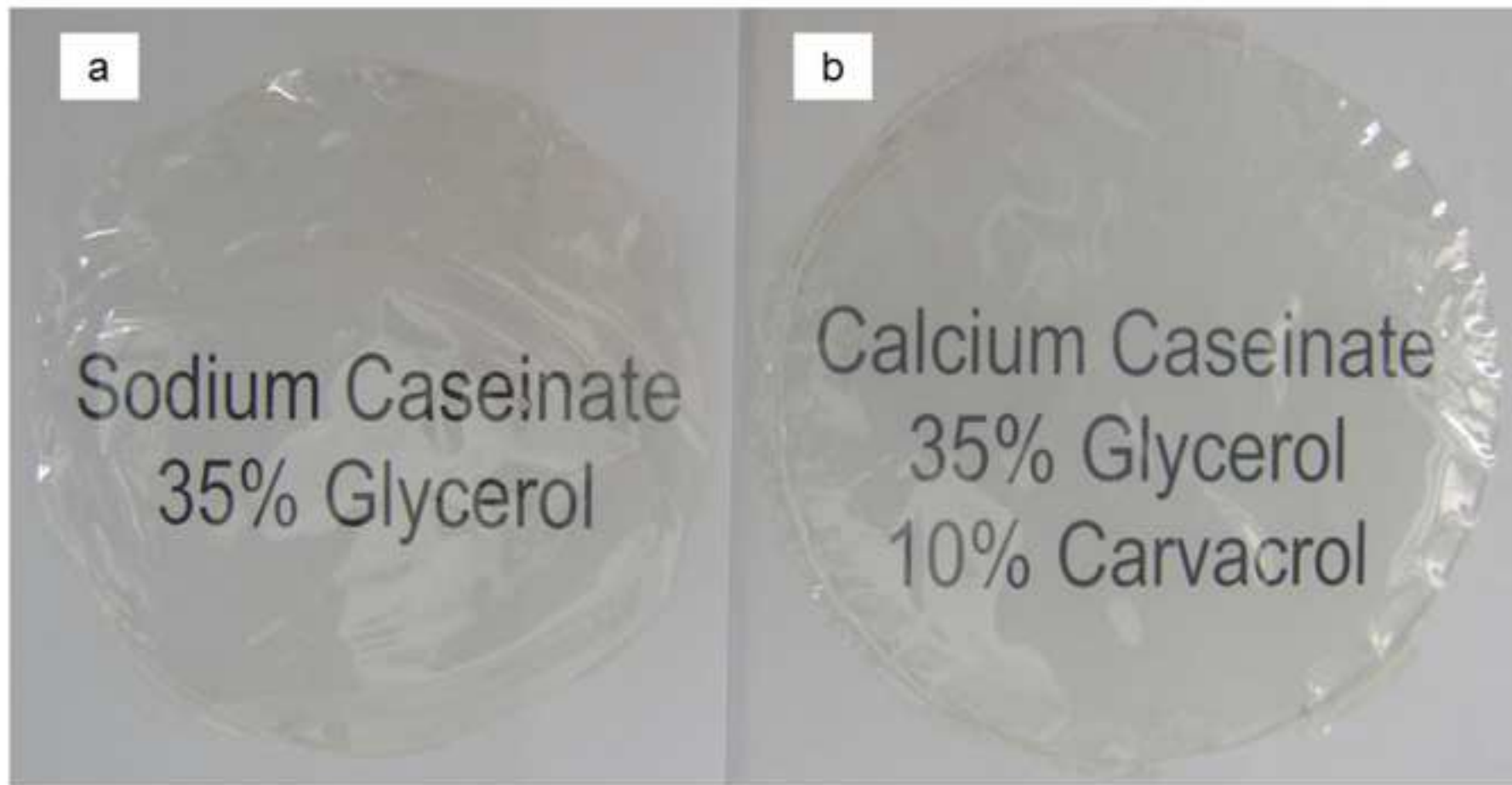
- 418 Arrieta, M.P., Parres García, F., López Martínez, J., Navarro Vidal, R., Ferrandiz, S.,
419 (2012). Pyrolysis of bioplastics waste: Obtained products from Poly(Lactic acid) (PLA).
420 DYNA 87(4), 395-399.
- 421 ASTM, (2001). Standard test method for tensile properties of thin plastic sheeting,
422 standards designation: D882-01 Annual book of ASTM standards. , Philadelphia, USA.
- 423 Audic, J.L., Chaufer, B., Daufin, G., (2003). Non-food applications of milk components
424 and dairy co-products: A review. Lait 83(6), 417-438.
- 425 Avena Bustillos, R.J., Krochta, J.M., (1993). Water vapor permeability of caseinate
426 based edible films as affected by pH, calcium cross-linking and lipid content. Journal of
427 Food Science 58(4), 904-907.
- 428 Barreto, P.L.M., Pires, A.T.N., Soldi, V., (2003). Thermal degradation of edible films
429 based on milk proteins and gelatin in inert atmosphere. Polymer Degradation and
430 Stability 79(1), 147-152.
- 431 Ben Arfa, A., Chrakabandhu, Y., Preziosi-Belloy, L., Chalier, P., Gontard, N., (2007).
432 Coating papers with soy protein isolates as inclusion matrix of carvacrol. Food
433 Research International 40(1), 22-32.
- 434 Cao-Hoang, L., Chaine, A., Gregoire, L., Wache, Y., (2010). Potential of nisin-
435 incorporated sodium caseinate films to control *Listeria* in artificially contaminated
436 cheese. Food Microbiology 27(7), 940-944.
- 437 Chalier, P., Ben Arfa, A., Preziosi-Belloy, L., Gontard, N., (2007). Carvacrol losses from
438 soy protein coated papers as a function of drying conditions. Journal of Applied
439 Polymer Science 106(1), 611-620.
- 440 Cho, S., Choi, Y., Park, S., Park, T., (2012). Carvacrol prevents diet-induced obesity by
441 modulating gene expressions involved in adipogenesis and inflammation in mice fed
442 with high-fat diet. Journal of Nutritional Biochemistry 23(2), 192-201.
- 443 Fabra, M.J., Talens, P., Chiralt, A., (2009). Microstructure and optical properties of
444 sodium caseinate films containing oleic acid-beeswax mixtures. Food Hydrocolloids
445 23(3), 676-683.

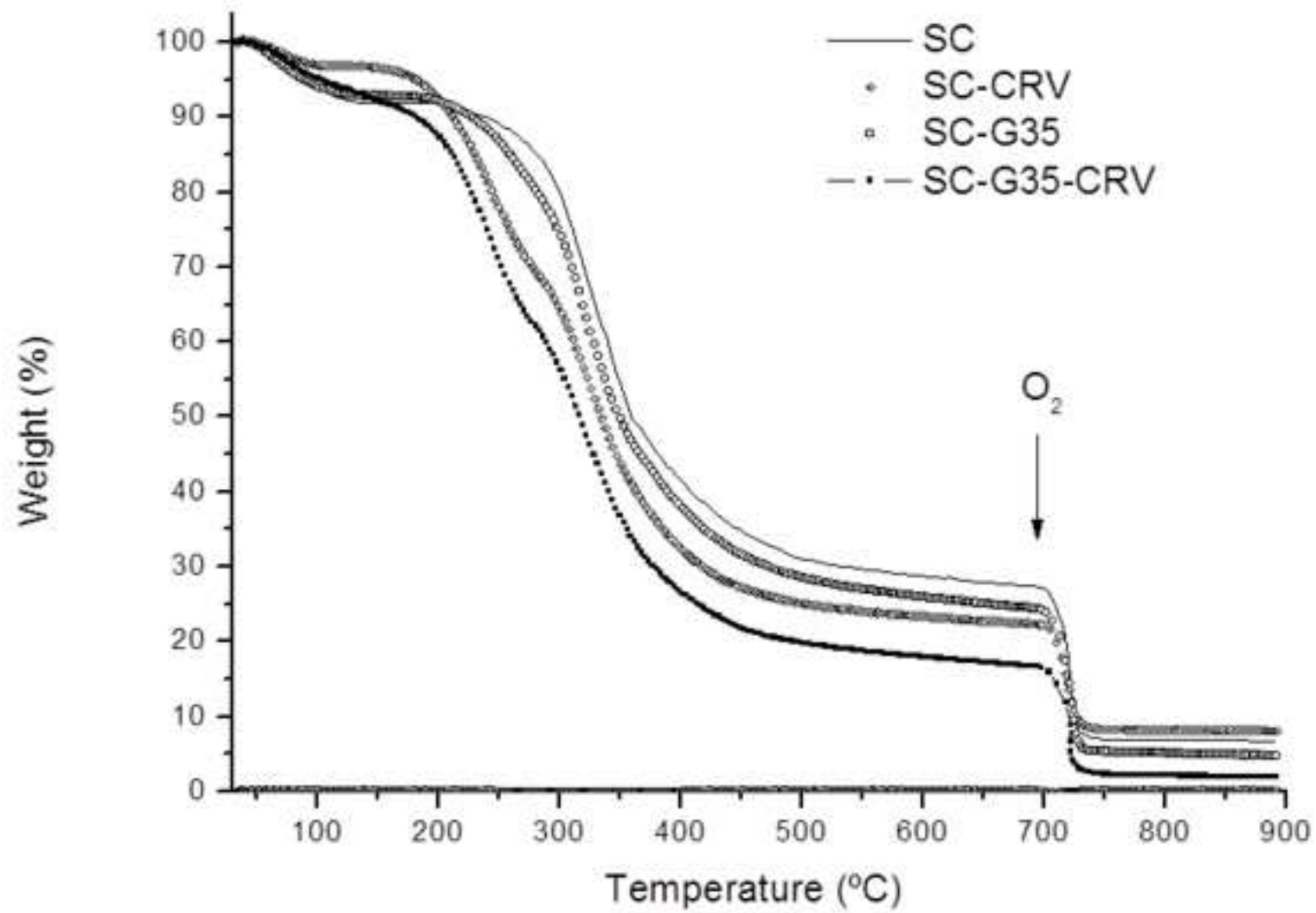
- 446 Fabra, M.J., Talens, P., Chiralt, A., (2010). Influence of calcium on tensile, optical and
447 water vapour permeability properties of sodium caseinate edible films. *Journal of Food*
448 *Engineering* 96(3), 356-364.
- 449 FDA Administration US
- 450 Fernandez, C., Ausar, S.F., Badini, R.G., Castagna, L.F., Bianco, I.D., Beltramo, D.M.,
451 (2003). An FTIR spectroscopy study of the interaction between alpha(s)-casein-bound
452 phosphoryl groups and chitosan. *International Dairy Journal* 13(11), 897-901.
- 453 Gastaldi, E., Chalier, P., Guillemain, A., Gontard, N., (2007). Microstructure of protein-
454 coated paper as affected by physico-chemical properties of coating solutions. *Colloids*
455 *and Surfaces a-Physicochemical and Engineering Aspects* 301(1-3), 301-310.
- 456 Gutierrez, L., Batlle, R., Sanchez, C., Nerin, C., (2010). New Approach to Study the
457 Mechanism of Antimicrobial Protection of an Active Packaging. *Foodborne Pathogens*
458 *and Disease* 7(9), 1063-1069.
- 459 Hasni, I., Bourassa, P., Hamdani, S., Samson, G., Carpentier, R., Tajmir-Riahi, H.-A.,
460 (2011). Interaction of milk alpha- and beta-caseins with tea polyphenols. *Food*
461 *Chemistry* 126(2), 630-639.
- 462 Hernandez-Izquierdo, V.M., Krochta, J.M., (2008). Thermoplastic processing of
463 proteins for film formation - A review. *Journal of Food Science* 73(2), R30-R39.
- 464 Jimenez, A., Fabra, M.J., Talens, P., Chiralt, A., (2012). Effect of sodium caseinate on
465 properties and ageing behaviour of corn starch based films. *Food Hydrocolloids* 29(2),
466 265-271.
- 467 Juvonen, H., Smolander, M., Boer, H., Pere, J., Buchert, J., Peltonen, J., (2011). Film
468 Formation and Surface Properties of Enzymatically Crosslinked Casein Films. *Journal*
469 *of Applied Polymer Science* 119(4), 2205-2213.
- 470 Kristo, E., Koutsoumanis, K.P., Biliaderis, C.G., (2008). Thermal, mechanical and water
471 vapor barrier properties of sodium caseinate films containing antimicrobials and their
472 inhibitory action on *Listeria monocytogenes*. *Food Hydrocolloids* 22(3), 373-386.

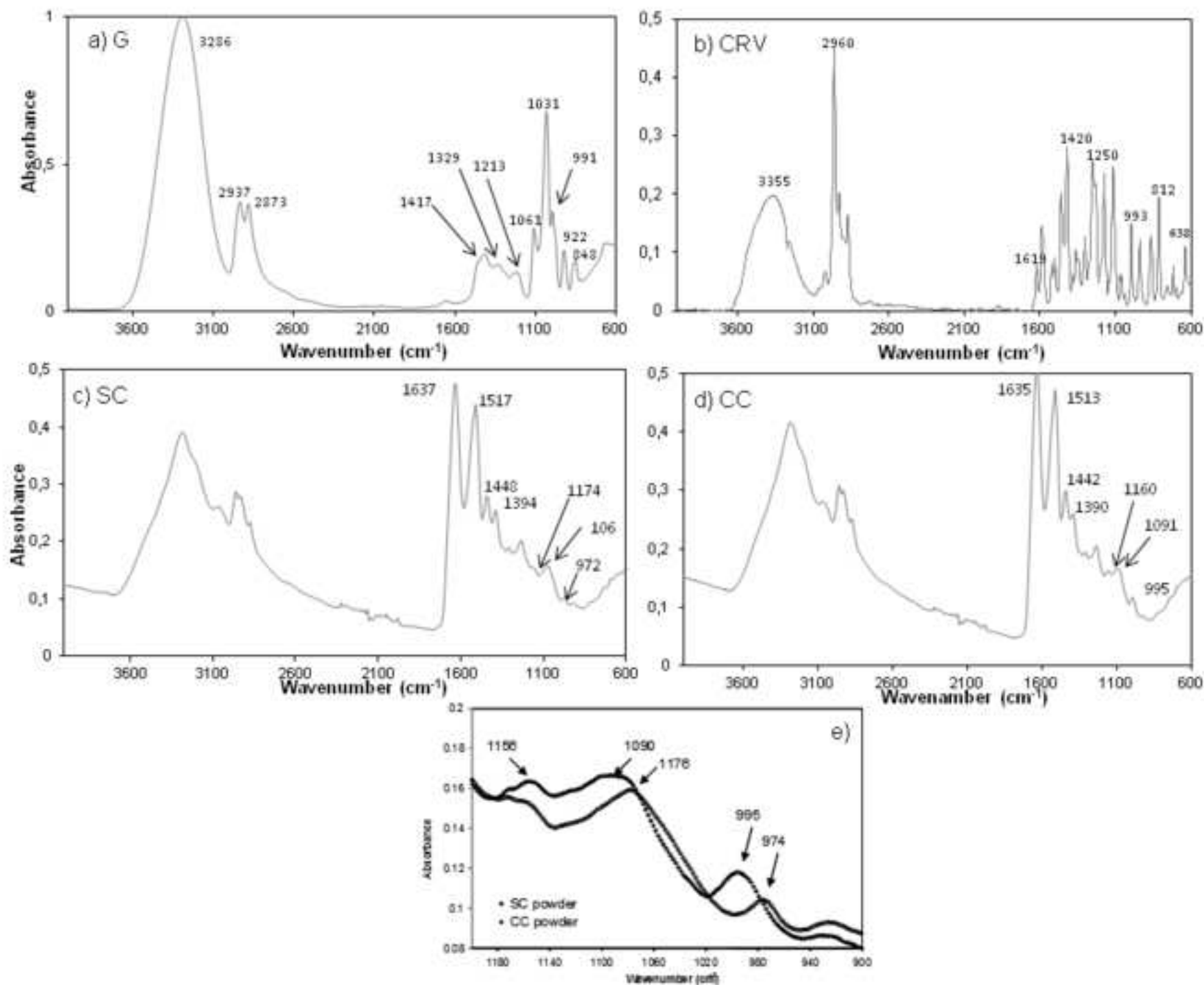
- 473 Lu, Y., Joerger, R., Wu, C., (2011). Study of the Chemical Composition and
474 Antimicrobial Activities of Ethanolic Extracts from Roots of *Scutellaria baicalensis*
475 Georgi. *Journal of Agricultural and Food Chemistry* 59(20), 10934-10942.
- 476 Martino, V.P., Ruseckaite, R.A., Jimenez, A., (2009). Ageing of poly(lactic acid) films
477 plasticized with commercial polyadipates. *Polymer International* 58(4), 437-444.
- 478 Mascheroni, E., Chalier, P., Gontard, N., Gastaldi, E., (2010). Designing of a wheat
479 gluten/montmorillonite based system as carvacrol carrier: Rheological and structural
480 properties. *Food Hydrocolloids* 24(4), 406-413.
- 481 Moreira, M.d.R., Pereda, M., Marcovich, N.E., Roura, S.I., (2011). Antimicrobial
482 Effectiveness of Bioactive Packaging Materials from Edible Chitosan and Casein
483 Polymers: Assessment on Carrot, Cheese, and Salami. *Journal of Food Science* 76(1),
484 M54-M63.
- 485 Nostro, A., Roccaro, A.S., Bisignano, G., Marino, A., Cannatelli, M.A., Pizzimenti, F.C.,
486 Cioni, P.L., Procopio, F., Blanco, A.R., (2007). Effects of oregano, carvacrol and thymol
487 on *Staphylococcus aureus* and *Staphylococcus epidermidis* biofilms. *Journal of*
488 *Medical Microbiology* 56(4), 519-523.
- 489 Oliver, C.M., Kher, A., McNaughton, D., Augustin, M.A., (2009). Use of FTIR and mass
490 spectrometry for characterization of glycated caseins. *Journal of Dairy Research* 76(1),
491 105-110.
- 492 Pelissari, F.M., Grossmann, M.V.E., Yamashita, F., Pineda, E.A.G., (2009).
493 Antimicrobial, Mechanical, and Barrier Properties of Cassava Starch-Chitosan Films
494 Incorporated with Oregano Essential Oil. *Journal of Agricultural and Food Chemistry*
495 57(16), 7499-7504.
- 496 Peltzer, M., Wagner, J., Jimenez, A., (2009). Migration study of carvacrol as a natural
497 antioxidant in high-density polyethylene for active packaging. *Food Additives and*
498 *Contaminants Part a-Chemistry Analysis Control Exposure & Risk Assessment* 26(6),
499 938-946.

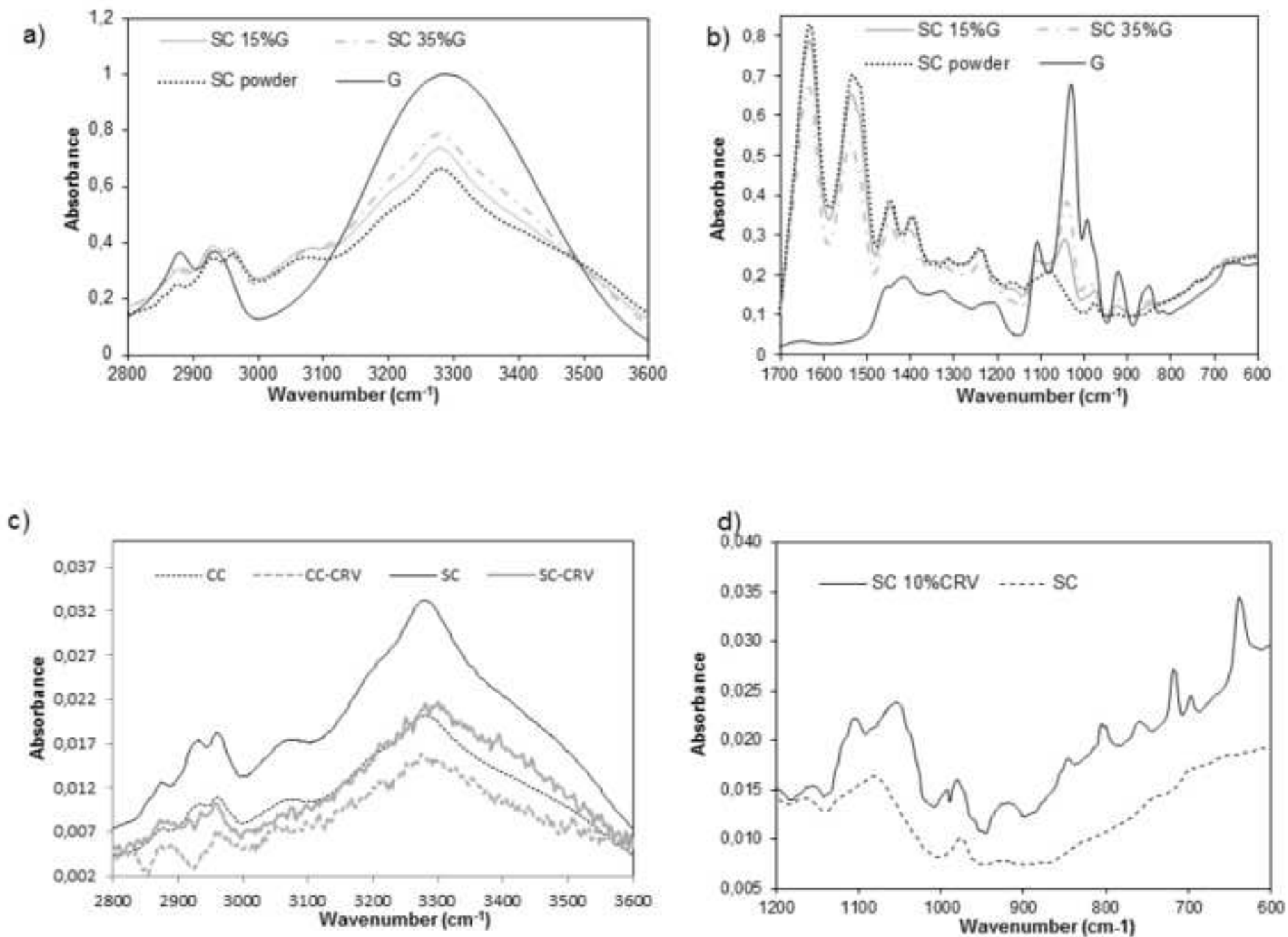
- 500 Pereda, M., Aranguren, M.I., Marcovich, N.E., (2008). Characterization of
501 chitosan/caseinate films. *Journal of Applied Polymer Science* 107(2), 1080-1090.
- 502 Pereda, M., Aranguren, M.I., Marcovich, N.E., (2010). Caseinate films modified with
503 tung oil. *Food Hydrocolloids* 24(8), 800-808.
- 504 Pereda, M., Ponce, A.G., Marcovich, N.E., Ruseckaite, R.A., Martucci, J.F., (2011).
505 Chitosan-gelatin composites and bi-layer films with potential antimicrobial activity. *Food*
506 *Hydrocolloids* 25(5), 1372-1381.
- 507 Persico, P., Ambrogi, V., Carfagna, C., Cerruti, P., Ferrocino, I., Mauriello, G., (2009).
508 Nanocomposite Polymer Films Containing Carvacrol for Antimicrobial Active
509 Packaging. *Polymer Engineering and Science* 49(7), 1447-1455.
- 510 Pojanavaraphan, T., Magaraphan, R., Chiou, B.-S., Schiraldi, D.A., (2010).
511 Development of Biodegradable Foamlike Materials Based on Casein and Sodium
512 Montmorillonite Clay. *Biomacromolecules* 11(10), 2640-2646.
- 513 Ponce, A.G., Roura, S.I., del Valle, C.E., Moreira, M.R., (2008). Antimicrobial and
514 antioxidant activities of edible coatings enriched with natural plant extracts: In vitro and
515 in vivo studies. *Postharvest Biology and Technology* 49(2), 294-300.
- 516 Pretsch, E., Bühlmann, P., Affolter, C., Herrera, A., & Martínez, R. , (2001).
517 Determinación estructural de compuestos orgánicos. . Springer-Verlag Ibérica.,
518 Barcelona.
- 519 Quintavalla, S., Vicini, L., (2002). Antimicrobial food packaging in meat industry. *Meat*
520 *Science* 62(3), 373-380.
- 521 Ramos, M., Jimenez, A., Peltzer, M., Garrigos, M.C., (2012). Characterization and
522 antimicrobial activity studies of polypropylene films with carvacrol and thymol for active
523 packaging. *Journal of Food Engineering* 109(3), 513-519.
- 524 Srinivasan, M., Singh, H., Munro, P.A., (1999). Adsorption behaviour of sodium and
525 calcium caseinates in oil-in-water emulsions. *International Dairy Journal* 9(3-6), 337-
526 341.

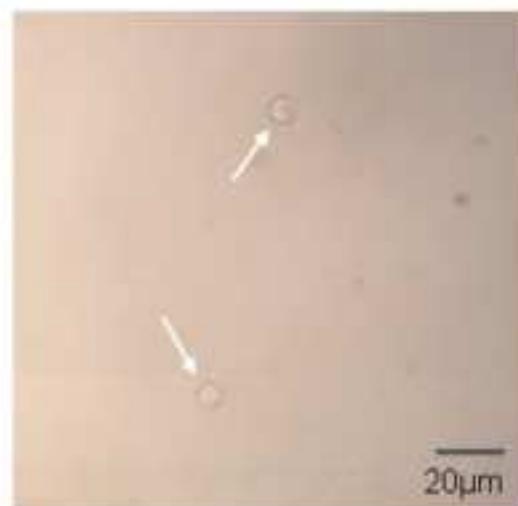
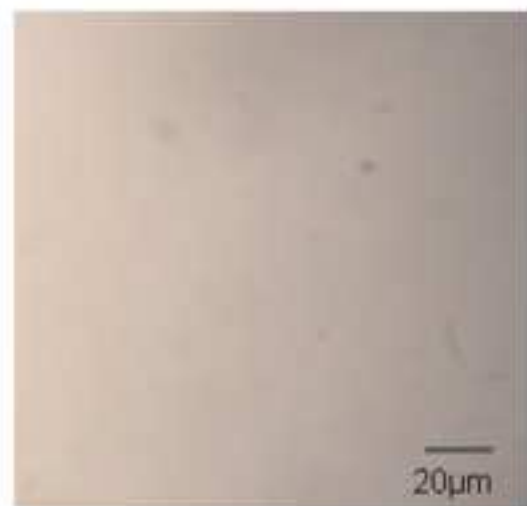
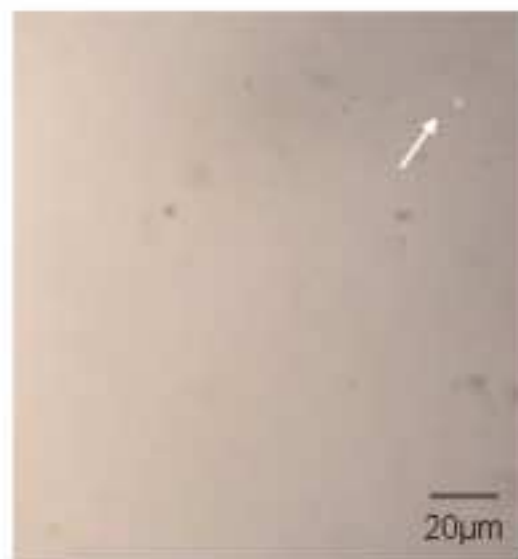
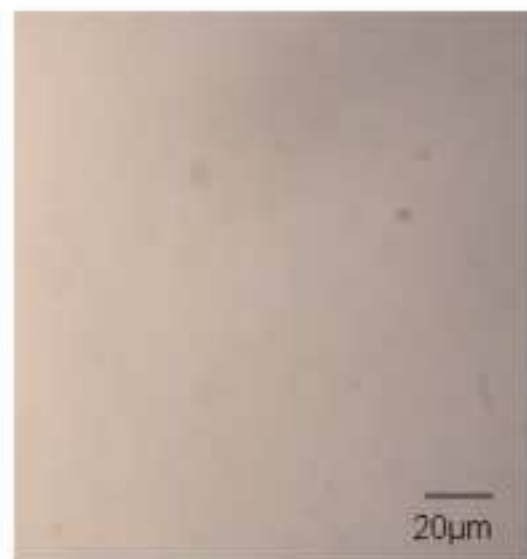
- 527 Ultee, A., Bennik, M.H.J., Moezelaar, R., (2002). The phenolic hydroxyl group of
528 carvacrol is essential for action against the food-borne pathogen *Bacillus cereus*.
529 *Applied and Environmental Microbiology* 68(4), 1561-1568.
- 530 Verbeek, C.J.R., Van den Berg, L.E., (2010). Extrusion Processing and Properties of
531 Protein-Based Thermoplastics. *Macromolecular Materials and Engineering* 295(1), 10-
532 21.
- 533 Viuda-Martos, M., El Gendy, A.E.-N.G.S., Sendra, E., Fernandez-Lopez, J., El Razik,
534 K.A.A., Omer, E.A., Perez-Alvarez, J.A., (2010). Chemical Composition and Antioxidant
535 and Anti-*Listeria* Activities of Essential Oils Obtained from Some Egyptian Plants.
536 *Journal of Agricultural and Food Chemistry* 58(16), 9063-9070.
- 537 Viuda-Martos, M., Mohamady, M.A., Fernandez-Lopez, J., Abd ElRazik, K.A., Omer,
538 E.A., Perez-Alvarez, J.A., Sendra, E., (2011). In vitro antioxidant and antibacterial
539 activities of essentials oils obtained from Egyptian aromatic plants. *Food Control*
540 22(11), 1715-1722.
- 541 Viuda-Martos, M., Ruiz-Navajas, Y., Fernandez-Lopez, J., Perez-Alvarez, J.A., (2007).
542 Antifungal activities of thyme, clove and oregano essential oils. *Journal of Food Safety*
543 27(1), 91-101.
- 544 Wang, N., Yu, J., Ma, X., Wu, Y., (2007). The influence of citric acid on the properties
545 of thermoplastic starch/linear low-density polyethylene blends. *Carbohydrate Polymers*
546 67(3), 446-453.
- 547 Ye, Z., Xiu, S., Shahbazi, A., Zhu, S., (2012). Co-liquefaction of swine manure and
548 crude glycerol to bio-oil: Model compound studies and reaction pathways. *Bioresource*
549 *Technology* 104, 783-787.

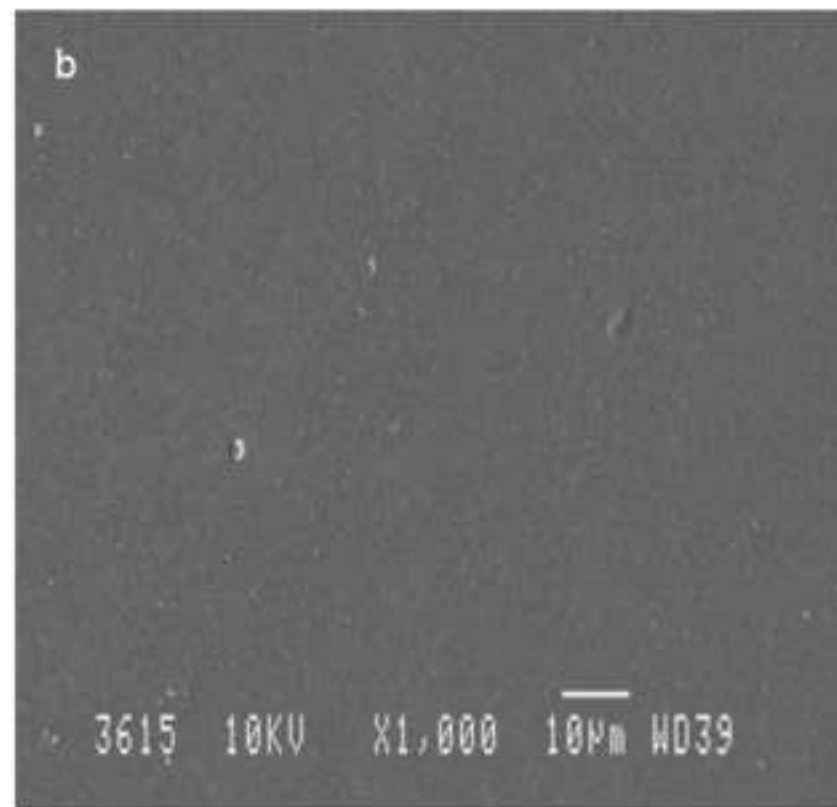
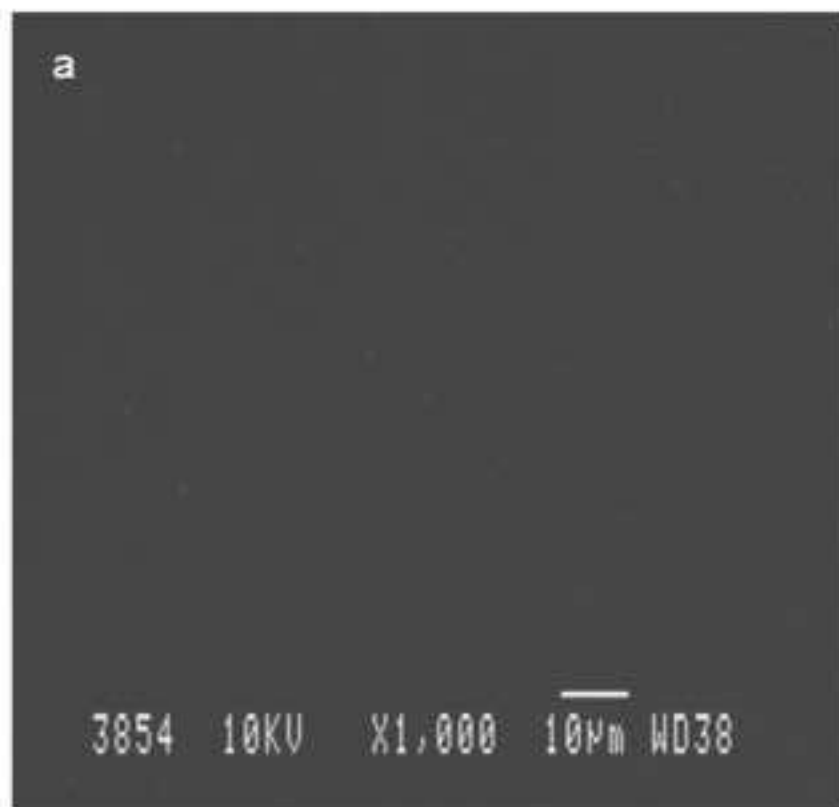


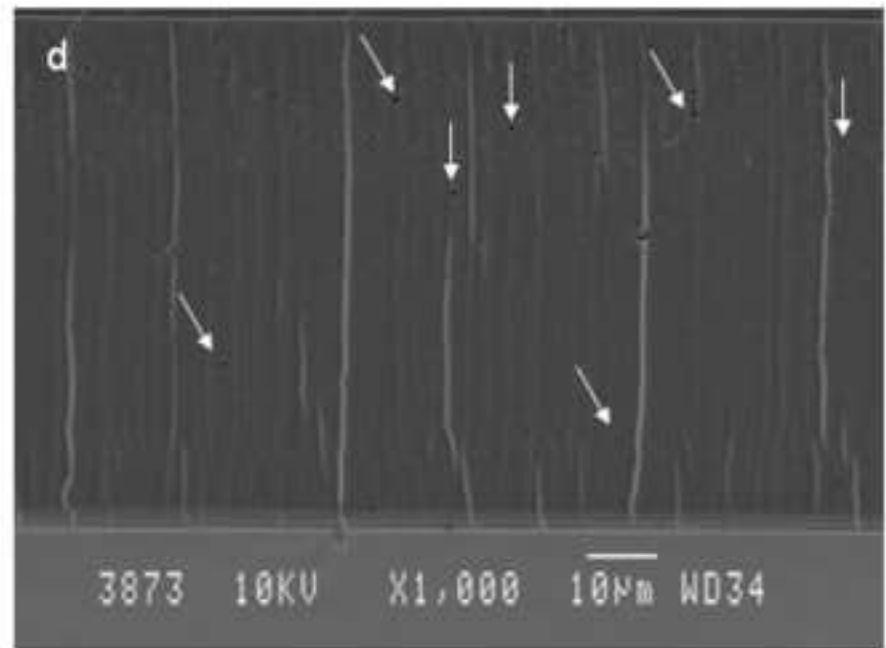
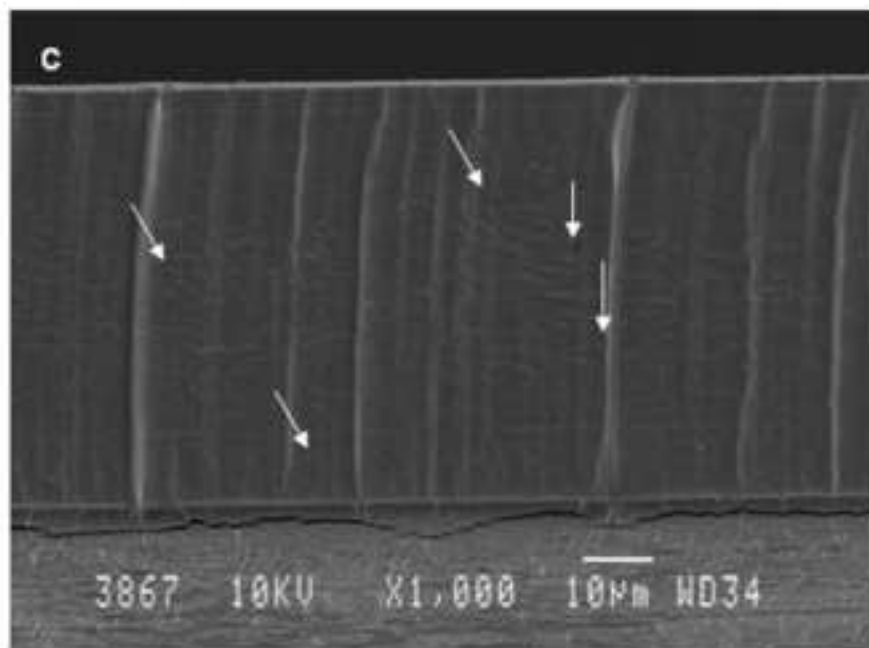
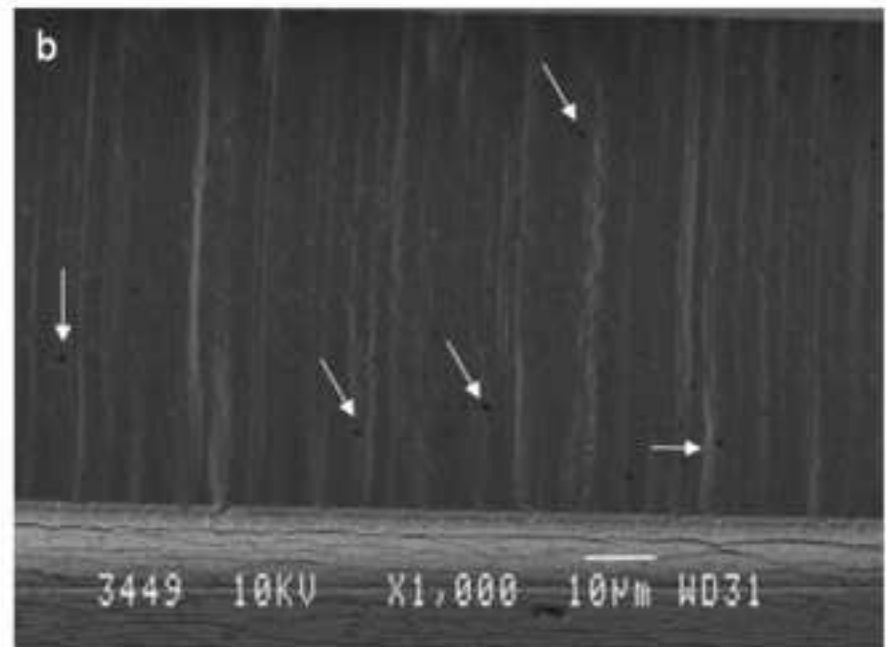
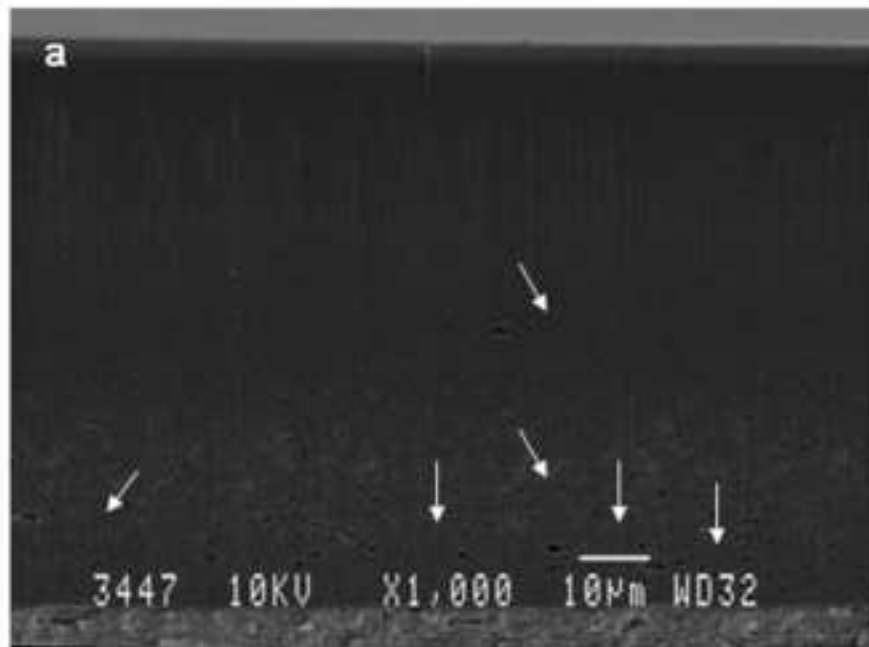












Captions to illustrations

Figure 1. Visual appearance of films based on: a) SC G35%, b) CC G35% CRV10%

Figure 2. Thermogravimetric curves of sodium caseinate (SC) edible films.

Figure 3. FTIR spectra of raw materials. a) G; b) CRV; c) SC, d) CC and d) SC + CC

Figure 4. a) and b) FTIR spectra of G, SC powered and SC edible films with two different concentration of glycerol ($3600-2800\text{ cm}^{-1}$ and $1700-600\text{ cm}^{-1}$ respectively); c) FTIR spectra of CC and SC films with and without CRV ($3600-2800\text{ cm}^{-1}$) and d) FTIR spectra of SC films with and without CRV ($1200-600\text{ cm}^{-1}$).

Figure 5. Optical micrograph (50x) of edible films surface: a) SC G35%, b) SC G35% CRV10%, c) CC G35% and d) CC G35% CRV10%.

Figure 6. SEM micrographs (1000x) of edible films surface: a) CC pure and b) CC G35% CRV10%.

Figure 7. SEM micrograph (1000x) of SC films cross section: a) SC unplasticized, b) SC G35%, c) SC G25% CRV10% and d) CC CRV10%

Table 1. Thermal parameters of SC samples obtained from TGA

Samples	Thermogravimetric parameters					
	T ₀ (°C)	Stage I		Stage II	Stage III	Residue at 900 °C (%)
		Interval (°C)	T _{max I} (°C)	T _{max II} (°C)	T _{max III} (°C)	
1:0:0	241	30-164	78	-	326	6.7
1:0.15:0	238	30-142	78	223	322	7.0
1:0.25:0	217	30-128	84	249	320	5.5
1:0.35:0	205	30-128	69	244	326	3.7
1:0:0.10	226	30-140	81	-	320	4.8
1:0.15:0.10	202	30-131	81	232	322	5.0
1:0.25:0.10	200	30-121	69	243	320	3.8
1:0.35:0.10	180	30-104	69	243	320	1.9

Table 2. Thermal parameters of CC samples obtained from TGA

Samples		Thermogravimetric parameters				Residue at 900 °C (%)
CC:G:CRV	T ₀ (°C)	Stage I		Stage II	Stage III	
		Interval (°C)	T _{max I} (°C)	T _{max II} (°C)	T _{max III} (°C)	
1:0:0	220	30-160	81	-	338	6.0
1:0.15:0	214	30-154	101	235	332	5.3
1:0.25:0	207	30-126	83	232	330	5.0
1:0.35:0	193	30-116	70	220	331	5.2
1:0:0.10	223	30-152	76	-	335	5.0
1:0.15:0.10	211	30-161	107	258	328	5.3
1:0.25:0.10	202	30-152	93	261	335	4.2
1:0.35:0.10	199	30-111	76	262	335	3.1

Table 3. Comparison between FTIR amide (1630 nm) and alcohol (1030 nm) bands of SC and CC samples

	SC:G:CRV					
	1:0.15:0	1:0.25:0	1:0.35:0	1:0.15:0.10	1:0.25:0.10	1:0.35:0.10
Amide I : alcohol 1°	1:0.23	1:0.36	1:0.49	1:0.54	1:0.61	1:0.83
	CC:G:CRV					
	1:0.15:0	1:0.25:0	1:0.35:0	1:0.15:0.10	1:0.25:0.10	1:0.35:0.10
Amide I : alcohol 1°	1:0.36	1:0.71	1:0.84	1:2.02	1:2.13	1:2.17

Table 4. Tensile properties of SC edible films ($n=5$)

SC:G:CRV	Tensile properties		
	ϵ_B (%)	E (MPa)	TS (MPa)
1:0.15:0	17 \pm 6	178 \pm 80	1.50 \pm 0.20
1:0.25:0	32 \pm 1	31 \pm 10	0.62 \pm 0.19
1:0.35:0	79 \pm 11	7 \pm 1	0.14 \pm 0.06
1:0.15:0.10	27 \pm 5	82 \pm 15	0.73 \pm 0.08
1:0.25:0.10	81 \pm 3	29 \pm 8	0.42 \pm 0.15
1:0.35:0.10	62 \pm 11	8 \pm 2	0.09 \pm 0.02

Table 5. Tensile properties of CC edible films ($n=5$)

CC:G:CRV	Tensile properties		
	ϵ_B (%)	E (MPa)	TS (MPa)
1:0.15:0	6 ± 2	424 ± 15	1.78 ± 0.09
1:0.25:0	9 ± 2	272 ± 6	0.54 ± 0.01
1:0.35:0	36 ± 2	39 ± 3	0.50 ± 0.02
1:0.15:0.10	5 ± 2	137 ± 2	3.02 ± 0.04
1:0.25:0.10	20 ± 3	61 ± 7	1.20 ± 0.05
1:0.35:0.10	33 ± 8	36 ± 6	0.26 ± 0.03

- Transparent and homogeneous edible active films based on caseinates were obtained.
- Sodium Caseinate films showed higher flexibility than the Calcium Caseinate ones.
- Glycerol and carvacrol showed good compatibility with caseinates to form films.

ACCEPTED MANUSCRIPT